Heat and Mass Transfer 36 (2000) 63–70 © Springer-Verlag 2000

Hydromagnetic simultaneous heat and mass transfer by mixed convection from a vertical plate embedded in a stratified porous medium with thermal dispersion effects

A. J. Chamkha, A.-R. A. Khaled

Abstract The problem of steady, laminar, hydromagnetic simultaneous heat and mass transfer by mixed convection flow over a vertical plate embedded in a uniform porous medium with a stratified free stream and taking into account the presence of thermal dispersion is investigated for the case of power-law variations of both the wall temperature and concentration. Certain transformations are employed to transform the governing differential equations to a local similarity form. The transformed equations are solved numerically by an efficient implicit, iterative, finite-difference scheme. The obtained results are checked against previously published work on special cases of the problem and are found to be in excellent agreement. A parametric study illustrating the influence of the magnetic field, porous medium inertia effects, heat generation or absorption, lateral wall mass flux, concentration to thermal buoyancy ratio, and the Lewis number on the fluid velocity, temperature and concentration as well as the Nusselt and the Sherwood numbers is conducted. The results of this parametric study is shown graphically and the physical aspects of the problem are discussed.

List of symbols

B	Mixed convection parameter ($B = \mathrm{Ra}_x/\mathrm{Pe}$)
B_o	Magnetic field strength
C	Concentration at any point in the flow field
C_∞	Concentration at the free stream
C_w	Concentration at the wall
D	Mass diffusivity
D_s	Porous medium thermal dispersion parameter ($D_s = \gamma u_\infty d/\alpha$)
e	Buoyancy ratio ($e = (\beta_\mathrm{c}(C_\mathrm{w} - C_\infty))/(\beta_\mathrm{T}(T_\mathrm{w} - T_\infty))$)
F	Inertia coefficient of the porous medium
f	Dimensionless stream function ($f = \psi/(\alpha\mathrm{Pe}^{1/2})$)
g	Gravitational acceleration
h	Local convective heat transfer coefficient
h_m	Local mass transfer coefficient
K	Permeability of the porous medium
k_e	Porous medium effective thermal conductivity
Le	Lewis number ($\mathrm{Le} = \alpha/D$)
M	Square of the Hartmann number ($M = (\sigma B_o K)/(\rho\upsilon)$)
Nu	Local Nusselt number ($\mathrm{Nu} = hx/k_\mathrm{e}$)
Pe	Local Peclet number ($\mathrm{Pe} = u_\infty x/\alpha$)
Q_o	Heat generation or absorption coefficient
Ra_x	Local Raleigh number ($\mathrm{Ra}_x = g\beta_\mathrm{T}K(T_\mathrm{w} - T_\infty)x/(\upsilon\alpha)$)
S	Stratification parameter
Sh	Local Sherwood number ($\mathrm{Sh} = h_\mathrm{m}x/D$)
T	Temperature at any point
T_w	Wall temperature
T_∞	Free stream temperature
u	Tangential or x-component of velocity
u_∞	Free stream velocity
v	Normal or y-component of velocity
V_o	Dimensionless wall mass transfer coefficient ($V_o = 2V_\mathrm{w}(x/(\alpha u_\infty))^{1/2}$)
V_w	Wall mass transfer velocity
x	Distance along the plate
y	Distance normal to the plate

Greek symbols

Γ	Dimensionless porous medium inertia coefficient ($\Gamma = (2FK)u_\infty/(\rho\upsilon)$)
α	Molecular thermal diffusivity
α_e	Effective thermal diffusivity of the porous medium
α_d	Thermal diffusivity of the porous medium due to thermal dispersion
β_c	Concentration expansion coefficient
β_T	Thermal expansion coefficient
δ	Dimensionless heat absorption parameter ($\delta = Q_o(x\alpha/u_\infty)$)
ϕ	Transformed concentration ($\phi = (C - C_\infty)/(C_\mathrm{w} - C_\infty)$)
γ	Thermal dispersion constant
η	Coordinate transformation in terms of x and y ($\eta = y/(x\mathrm{Pe}^{1/2})$)
υ	Fluid kinematic viscosity
ψ	Stream function
θ	Transformed temperature ($\theta = (T - T_\infty)/(T_\mathrm{w} - T_\infty)$)
ρ	Fluid density
σ	Fluid electrical conductivity

Received on 17 November 1998

A. J. Chamkha, A.-R. A. Khaled
Department of Mechanical and Industrial Engineering
Kuwait University P.O. Box 5969 Safat, 13060 Kuwait

1 Introduction

Simultaneous heat and mass transfer from different geometries embedded in porous media has many engineering and geophysical applications such as geothermal reservoirs, drying of porous solids, thermal insulation,

enhanced oil recovery, packed-bed catalytic reactors, cooling of nuclear reactors, and underground energy transport. Most early studies on porous media have used the Darcy law which is a linear empirical relation between the Darcian velocity and the pressure drop across the porous medium and is limited to slow flows. However, for high velocity flow situations, the Darcy law is inapplicable since it does not account for the resulting inertia effects of the porous medium. In this situation, the relation between the velocity and the pressure drop is quadratic. The high flow situation is established when the Reynolds number based on the pore size is greater than unity. Vafai and Tien (1981) have discussed the importance of inertia effects for flows in porous media. More recently, Lai (1991) has investigated coupled heat and mass transfer by mixed convection from an isothermal vertical plate in a porous medium.

Cheng and Minkowycz (1977) have presented similarity solutions for free thermal convection from a vertical plate in a fluid-saturated porous medium. The problem of combined thermal convection from a semi-infinite vertical plate in the presence or absence of a porous medium has been studied by many authors (see, for example, Mikowycz et al., 1985; Ranganathan and Viskanta, 1984; Nakayama and Koyama, 1987; Hsieh, 1993). Nakayama and Koyama (1987) have suggested similarity transformations for pure, combined and forced convection in Darcian and non-Darcian porous media. Hsieh (1993) has presented non-similar solutions for combined convection in porous media. Gorla et al. (1996) have studied the effects of free stream thermal stratification and thermal dispersion on combined convection over a vertical plate embedded in a uniform porous medium. Chamkha (1997a) has investigated hydromagnetic natural convection from a isothermal inclined surface adjacent to a thermally stratified porous medium.

A secondary effect of a porous medium on the flow appears as a result of mixing and recirculation of local fluid particles through tortuous paths formed by the porous medium solid particles. This effect is classified as thermal dispersion (see Amiri and Vafai, 1994). Plumb (1983) modeled thermal dispersion effects over a vertical plate as linear increases of a fluid thermal diffusivity with the increases in the tangential flow velocity. In their model, Amiri and Vafai (1994) have shown that the thermal diffusivity of the fluid is also proportional the free stream Reynolds number based on the porous medium pore diameter. Other works dealing with thermal dispersion effects in porous media can be found in the papers by Tien (1988) and Cheng and Vortmeyer (1988).

There has been a renewed interest in studying magnetohydrodynamic (MHD) flow and heat transfer in porous and non-porous media due to the effect of magnetic fields on the flow control and on the performance of many systems using electrically-conducting fluids. For example, Rapits et al. (1982) have analyzed hydromagnetic free convection flow through a porous medium between two parallel plates. Aldoss et al. (1995) have studied mixed convection from a vertical plate embedded in a porous medium in the presence of a magnetic field. Bian et al. (1995) have reported on the effect of an electromagnetic field on natural convection in an inclined porous medium. Buoyancy-driven convection in a rectangular enclosure with a transverse magnetic field has been considered by Garandet et al. (1992) and Khanafer and Chamkha (1998).

In certain porous media applications such as those involving heat removal from nuclear fuel debris, underground disposal of radioactive waste material, storage of food stuffs, and exothermic chemical reactions and dissociating fluids in packed-bed reactors, the working fluid heat generation (source) or absorption (sink) effects are important. Representative studies dealing with these effects have been reported by such authors as Acharya and Goldstein (1985), Vajravelu and Nayfeh (1992) and Chamkha (1996, 1997b).

The objective of this paper is to consider simultaneous heat and mass transfer by mixed convection from a vertical plate embedded in a fluid-saturated porous medium in the presence of mass blowing or suction, magnetic field effects, heat generation or absorption effects, free stream thermal stratification, porous medium inertia and thermal dispersion effects. This will be done for power-law variations of both the wall temperature and concentration. It should be noted that the above problem would provide some insight into assessment and evaluation of geothermal resources and can help in developing advanced technologies for nuclear waste management. These applications and others are mentioned in the work of Rathish and Singh (1998) where they studied the effect of thermal stratification on free convection in a fluid-saturated porous enclosure.

2
Problem formulation

Consider steady, laminar, hydromagnetic coupled heat and mass transfer by mixed convection flow over a semi-infinite permeable vertical plate embedded in a fluid-saturated porous medium. Figure 1 shows the schematic diagram and coordinate system of the problem. A magnetic field of uniform strength B_o is applied in the y-direction that is normal to the plate. The fluid is assumed to be Newtonian, electrically conducting, heat generating or absorbing and has constant properties except the

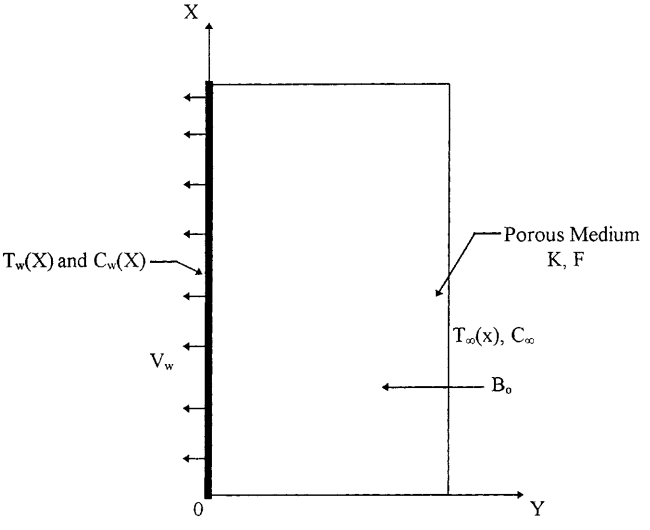

Fig. 1.

density in the buoyancy terms of the balance of linear momentum equation. Also, the porosity and the permeability of the porous medium are assumed to be constant. The fluid and the porous medium are assumed to be in local thermal equilibrium. Both the wall temperature and concentration are assumed to have power-law variations with the vertical distance along the plate x. The free stream temperature is also assumed to be stratified with a power-law variation with x. However, the concentration of the free stream is assumed to be constant. The temperature and the concentration at the plate surface are always greater than the free stream values existing far from the plate surface. The magnetic Reynolds number is assumed to be small so that the induced magnetic field can be neglected. In addition, there is no applied electric field and the Hall effect, Joule heating and viscous dissipation are all neglected in this work.

The governing equations which take into account the inertia and thermal dispersion effects of the porous medium within the boundary layer in addition to the Boussinesq approximation may be written as follows:

$$\frac{\partial u}{\partial x}+\frac{\partial v}{\partial y}=0 \tag{1}$$

$$\left(1+\frac{\sigma B_o^2 K}{\rho \upsilon}+\frac{2FK}{\rho\upsilon}u\right)\frac{\partial u}{\partial y}=\frac{g\beta_T K}{\upsilon}\frac{\partial T}{\partial y}+\frac{g\beta_c K}{\upsilon}\frac{\partial C}{\partial y} \tag{2}$$

$$u\frac{\partial T}{\partial x}+v\frac{\partial T}{\partial y}=\frac{\partial}{\partial y}\left(\alpha_e\frac{\partial T}{\partial y}\right)+\frac{Q_o}{\rho c_p}(T-T_\infty) \tag{3}$$

$$u\frac{\partial C}{\partial x}+v\frac{\partial C}{\partial y}=D\frac{\partial^2 C}{\partial y^2} \tag{4}$$

where u, v, T and C are the fluid x-component of velocity, y-component of velocity, temperature, and concentration, respectively. u and v become the Darcian velocities when the porous medium inertia coefficient F is set of zero. $\rho, \upsilon, c_p, \beta_T$, and β_c are the fluid density, kinematic viscosity, specific heat at constant pressure, coefficient of thermal expansion, and coefficient of concentration expansion, respectively. σ, Q_o, and D are the fluid electrical conductivity, heat generation (>0) or absorption (<0) coefficient, and mass diffusivity, respectively. g and B_o are the gravitational acceleration and magnetic induction, respectively. K and α_e are the porous medium permeability and the effective thermal diffusivity, respectively.

It should be noted that in general Eqs. (1)–(4) are coupled with Maxwell's equations (charge, current, and magnetic field continuity equations, Ampere's law and Faraday's law). However, for small magnetic Reynolds numbers as considered in this work this will not be the case. The magnetic boundary-layer phenomenon occurs when the influence of a physical quantity is restricted to a small region near a confining boundary. This phenomenon occurs when the magnetic Reynolds number is large and the magnetic boundary layer thickness is inversely proportional to the square root of the magnetic Reynolds number. For a small magnetic Reynolds number as is the case in many physical situations, the thickness of the magnetic boundary-layer is very large and the induced magnetic field is negligible. Therefore, by applying a uniform transverse magnetic field normal to the flow direction under the small magnetic Reynolds number assumption and in the absence of an electric field, Maxwell's equations are identically satisfied are uncoupled from the momentum and energy equations (see Cramer and Pai, 1973).

The boundary conditions for this problem can be written as

$$y=0\text{: } v=V_w(x),\quad T=T_w(x),\quad C=C_w(x) \tag{5}$$

$$y\to\infty\text{: } u=u_\infty,\quad T=T_\infty(x),\quad C=C_\infty \tag{6}$$

where all of the wall temperature T_w, wall concentration C_w and the free stream temperature T_∞ vary along the plate according to the following power-law functions:

$$T_w-T_\infty=Ax^\lambda,\quad C_w-C_\infty=Ax^\lambda,\quad T_\infty-T_o=SAx^\lambda \tag{7}$$

In Eqs. (5)–(7), V_w is the surface mass transfer coefficient, u_∞, T_∞ and C_∞ are the free stream velocity, temperature and concentration, respectively. T_o, A, λ and S are constants.

In situations of fluid flow and heat transfer in porous media, the effective thermal diffusivity is modeled by Yagi et al. (1964) and later by Plumb (1983) according to

$$\alpha_e=\alpha+\alpha_d \tag{8}$$

where α and α_d are the molecular and thermal dispersion thermal diffusivities of the fluid and the porous medium, respectively. Yagi et al. (1964) and Plumb (1983) represented α_d as a linear relation of the fluid velocity as follows

$$\alpha_d=\gamma u d \tag{9}$$

where d is the mean particle diameter and γ is a constant. Gorla et al. (1996) have used the same model. Since the present problem represents a generalization to the problem of Gorla et al. (1996) and in order to allow for comparisons, the same model used in the present work.

Invoking the following dimensionless variables which were reported earlier by Gorla et al. (1996):

$$\eta=\frac{y}{x}\mathrm{Pe}^{1/2} \tag{10}$$

$$f(\xi,\eta)=\frac{\psi}{\alpha\mathrm{Pe}^{1/2}} \tag{11}$$

$$\theta(\xi,\eta)=\frac{T-T_\infty}{T_w-T_\infty} \tag{12}$$

$$\phi(\xi,\eta)=\frac{C-C_\infty}{C_w-C_\infty} \tag{13}$$

where ψ is the dimensional stream function, $\mathrm{Ra}_x=g\beta_T K(T_w-T_\infty)x/(\upsilon\alpha)$ is the local Rayleigh number and $\mathrm{Pe}=u_\infty x/\alpha$ is the local Peclet number, results in the following local similarity equations

$$(1+M+\Gamma f')f''=B(\theta'+e\phi') \tag{14}$$

$$(1+D_s f')\theta''+\left(D_s f''+\frac{1}{2}f\right)\theta'+(\delta-\lambda f')\theta-\lambda f' S=0 \tag{15}$$

$$\frac{1}{\mathrm{Le}}\phi'' + \frac{1}{2}f\phi' - \lambda f'\phi = 0 \tag{16}$$

where

$$M = \frac{\sigma B_o^2 K}{\rho \upsilon}, \quad \Gamma = \frac{2FKu_\infty}{\rho\upsilon}, \quad e = \frac{\beta_c(C_w - C_\infty)}{\beta_T(T_w - T_\infty)} \tag{17}$$

$$\mathrm{Le} = \frac{\alpha}{D}, \quad \delta = Q_o\left(\frac{x\alpha}{u_\infty}\right), \quad B = \frac{\mathrm{Ra}_x}{\mathrm{Pe}}, \quad D_s = \frac{\gamma u_\infty d}{\alpha} \tag{18}$$

are the square of the Hartmann number, dimensionless porous medium inertia coefficient, buoyancy ratio, Lewis number, dimensionless internal heat generation or absorption parameter, mixed convection parameter and the porous medium thermal dispersion parameter, respectively. In Eq. (14), $B = 0$, corresponds to the forced convection regime and as B becomes large the free convection regime dominates.

After transformation, the boundary conditions become

$$\eta = 0: f = V_o, \quad \theta = 1, \quad \phi = 1 \tag{19}$$

$$\eta \to \infty: f' = 1, \quad \theta = 0, \quad \phi = 0 \tag{20}$$

where $V_o = 2V_w(x/(\alpha u_\infty))^{1/2}$ is the dimensionless wall mass transfer coefficients. To eliminate x from δ and V_o, Q_o must be selected such that it is inversely proportional to the distance along the plate and the normal velocity at the surface V_w must be inversely proportional to the square root of x. If the Rayleigh number is fixed, then the resulting equations will be similar at a fixed value of x (since Ra_x is a function of x). Therefore, Eqs. (14)–(16) represent locally similar equations. It should be mentioned here that, in the absence of heat generation or absorption, Eq. (15) is slightly different from the corresponding equation derived by Gorla et al. (1996) by a single term. The term $\lambda f\theta'$ appearing in Eq. (10) in the paper by Gorla et al. (1996) appears to be a mistake as this term is not obtained during the transformation of the governing equations.

The local Nusselt and Sherwood numbers are important physical characteristics for this flow and heat transfer situation. These are defined as follows:

$$\mathrm{Nu} = \frac{hx}{k_e} = -\theta'(0)\mathrm{Ra}_x^{1/2} \tag{21}$$

$$\mathrm{Sh} = \frac{h_m x}{D} = -\phi'(0)\mathrm{Ra}_x^{1/2} \tag{22}$$

where h, k_e and h_m are the convective heat transfer coefficient, effective thermal conductivity and the convective mass transfer coefficient, respectively.

3 Numerical method

The implicit finite-difference method discussed by Blottner (1970) has proven to be accurate and adequate for the solution of differential equations similar to Eqs. (14)–(16). For this reason, it is employed in the present work. These equations have been linearized and then descritized using three points central difference quotients with variable step sizes in the η direction. The resulting equations form a tri-diagonal system of algebraic equations that can be solved by the well known Thomas algorithm (see Blottner, 1970). Due to nonlinearities of the equations, an iterative solution is required. For convergence, the maximum absolute error between two successive iterations was taken to be 10^{-7}. A starting step size of 0.001 in the η direction with an increase of 1.03 times the previous step size was found to give accurate results. The total number of points in the η direction was taken to be 499 to ensure proper approach of the solution to the free stream conditions. The accuracy of the aforementioned numerical method was validated by direct comparisons with the numerical results reported earlier by Gorla et al. (1996) for the cases $S = 0.5$, $\lambda = 0$ and $D_s = 0$ and in the absence of magnetic, heat generation or absorption, mass blowing or suction, porous medium inertia and concentration buoyancy effects since in this case the local similarity equations of Gorla et al. (1996) and those of the present work are the same. Table 1 presents the results of the these comparisons. It can be seen from the table that excellent agreement between the results exists. These favorable comparisons lend confidence in the numerical results to be reported in the next section.

4 Results and discussion

Figures 2 and 3 present the behavior of the velocity and the temperature profiles for the cases represented in Table 2 at $B = S = \lambda = 1.0$ and $D_s = 0$. The presence of a magnetic field in an electrically conducting fluid tends to produce a

Table 1. Values for $f'(0)$ and $-\theta'(0)$ (for $D_s = 0$, $e = 0$, $M = 0$, $S = 0.5$, $V_o = 0$, $\Gamma = 0$, $\delta = 0$ and $\lambda = 0$)

B	Gorla et al. (1996)		Present work	
	$f'(0)$	$-\theta'(0)$	$f'(0)$	$-\theta'(0)$
0.0	1.0000	0.58398	1.0000	0.5644
1.0	2.0000	0.72875	1.9994	0.7207
2.0	3.0000	0.85160	2.9983	0.8477
5.0	6.0000	1.14639	5.9936	1.1454
10.0	11.000	1.51638	10.982	1.5156
20.0	21.000	2.06634	20.947	2.0645

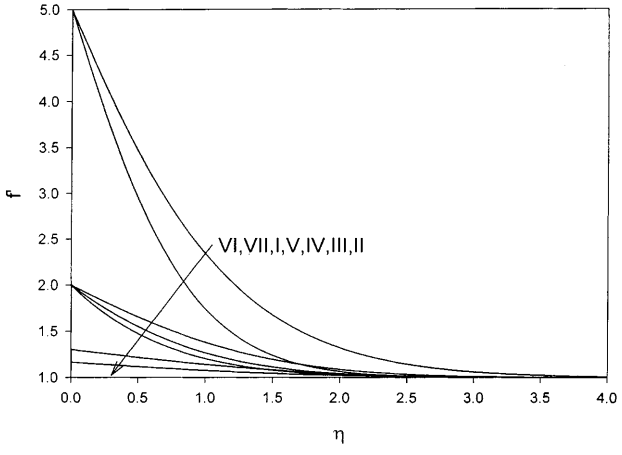

Fig. 2.

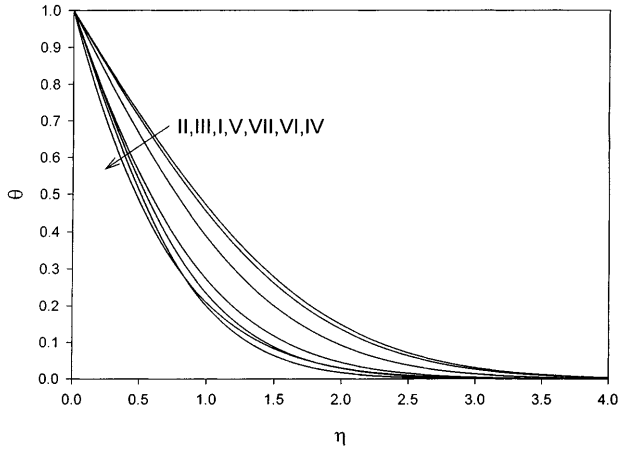

Fig. 3.

body force against the flow. This type of resistive force tend to slow down the flow which, in turn, reduces the rate of heat convection in the flow and this appears in increasing the flow temperatures as shown in curve II compared to the reference curve I in both figures. Additional resistance against the flow occurs if the porous medium inertia effect is considered especially at high flow velocities. As a result, the velocity near the wall decreases while the flow temperature increases as depicted from curve III when compared with curve I. Curve IV shows the effect of internal heat absorption on both the velocity and temperature profiles. The value of $\delta = -1.5$ represents a large value of a heat sink that causes the temperature of the fluid to reduce to the free stream temperature at a rapid rate as shown in curve IV in Fig. 3. This, in turn, reduces the thermal buoyancy forces causing a reduction in the velocity profile. Accordingly, the hydrodynamic boundary-layer thickness will be very small. The presence of wall mass suction represented by curve V has the effect of decreasing the boundary-layer thickness and increasing the rate of heat convection which results in decreasing both the velocity and temperature profiles. Including mass diffusion effects increases the flow velocity and decreases its temperature due to additional concentration buoyancy forces. This is obvious from curves VI and VII which correspond to different Lewis numbers compared to curve I in which concentration buoyancy forces are excluded.

Figure 4 illustrates the effects of the thermal stratification parameter S and the power index λ on the local Nusselt number $\mathrm{NuRa}_x^{-1/2}$. It is noticed that the Nusselt number increases as both S and λ increase. Physically, positive values of the stratification parameter have the tendency to decrease the boundary-layer thickness due to the reduction in the temperature difference between the wall and the free stream. This causes increases in the Nusselt number as shown in Fig. 4. The increase in the Nusselt number as λ increases is due to the increase in the wall temperature gradient which increases the thermal convective energy.

Figures 5–8 show the effects of the square of the Hartmann number M, porous medium inertia coefficient Γ, dimensionless internal heat generation or absorption parameter δ and the dimensionless mass blowing or suction parameter V_o on the local Nusselt number. From Fig. 3, it is noticed that the flow temperature increases while its absolute wall slope decreases as M, Γ and δ increase and decreases as V_o increases. This has the direct effect in reducing the local Nusselt number for the increases in the values of all of M, Γ and δ and for the decrease in the value of V_o. It should be mentioned here that for positive values of δ the numerical method does not converge for the parametric values employed. This indicates that the equations become stiff for this case. For this reason, no results are shown for the case of heat generation.

Figure 9 illustrates the effects of the porous medium thermal dispersion parameter D_s and the power index λ on

Table 2. Parmetric values for the curves in Figs. 2 and 3

Curve	e	Le	V_o	M	Γ	δ
I	0	0	0	0	0	0
II	0	0	0	5	0	0
III	0	0	0	0	2	0
IV	0	0	0	0	0	−1.5
V	0	0	1	0	0	0
VI	3	0.5	0	0	0	0
VII	3	1.25	0	0	0	0

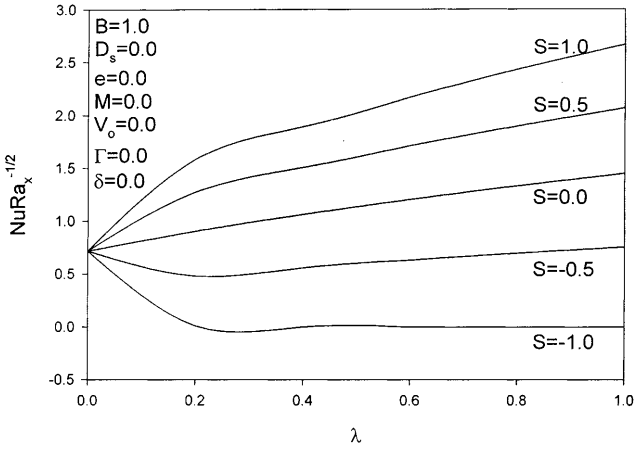

Fig. 4.

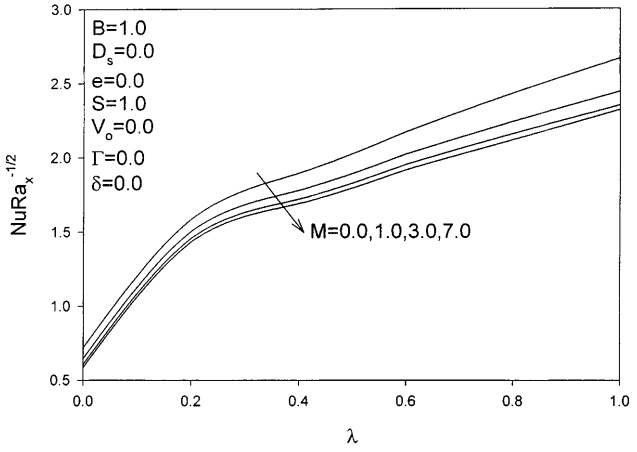

Fig. 5.

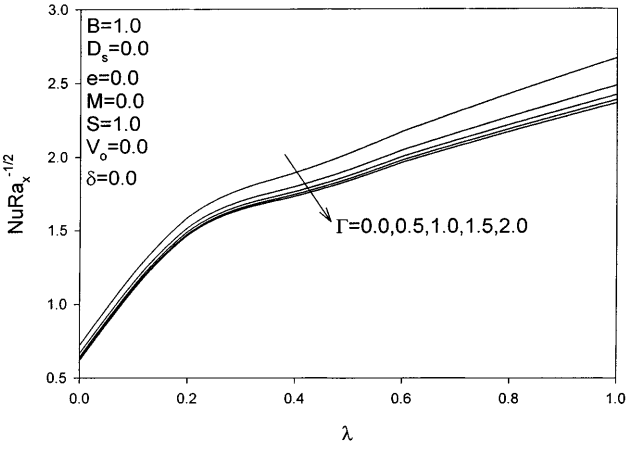

Fig. 6.

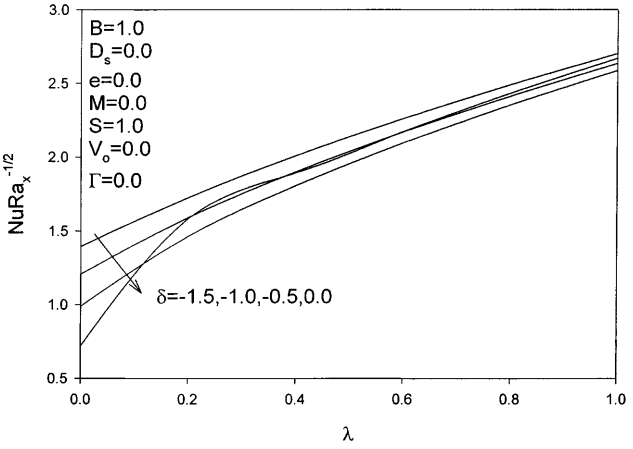

Fig. 7.

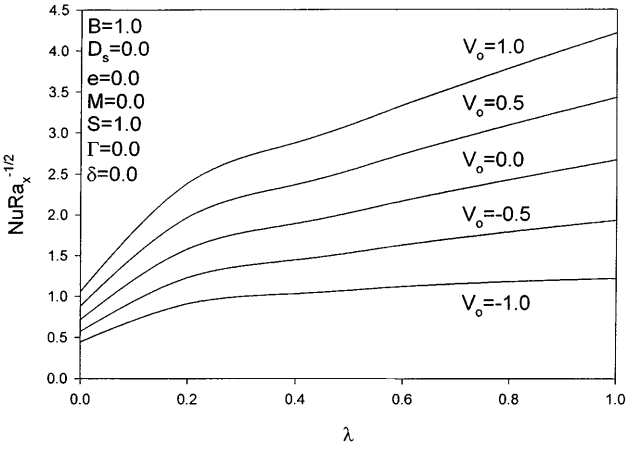

Fig. 8.

the local Nusselt number. Increasing the thermal dispersion parameter results in an increase in the thermal diffusion and, as a result the velocity increases. This, in turn, results in increasing the rate of heat extracted from the plate. Figure 9 shows that the local Nusselt number de-

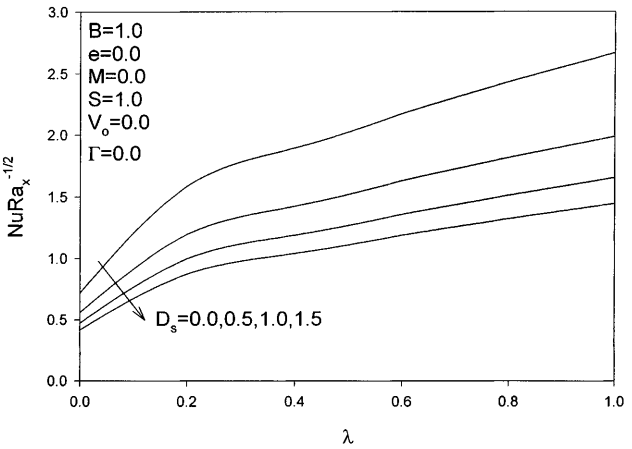

Fig. 9.

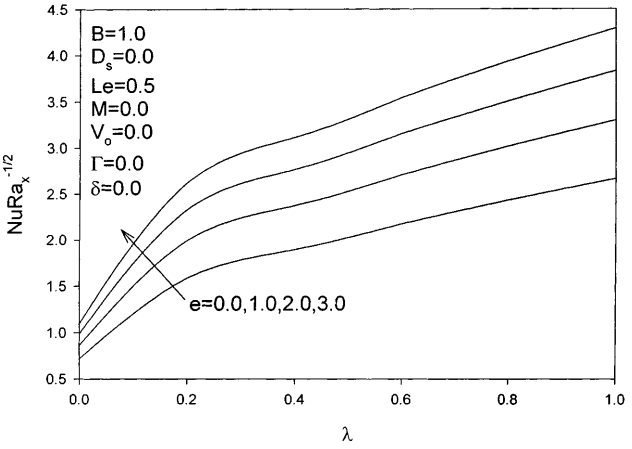

Fig. 10.

creases as D_s increases. Since the wall heat flux is a function of both the local Nusselt number and the porous medium effective thermal conductivity. Therefore, Fig. 9 is not expected to represent the effect of thermal dispersion on the wall heat flux.

Figures 10–13 show the effects of *e* and Le on the local Nusselt and Sherwood numbers, respectively. It is observed from Fig. 3 that the absolute wall temperature slope is increased as a result of the increase in *e* and the decrease in Le. This causes an increase in the Nusselt number and similarly for the Sherwood number, since energy and concentration equation are similar, when *e* is increased as is clear from Figs. 10 and 11. However, increasing the value of Le causes a reduction in the values of the local Nusselt number and an increase in the values of the local Sherwood number as shown in Figs. 12 and 13.

5 Conclusion

The problem of steady, laminar, simultaneous heat and mass transfer by mixed convection boundary-layer flow of an electrically-conducting and heat absorbing fluid over a permeable vertical plate embedded in a uniform porous medium with thermal dispersion was considered. All of the

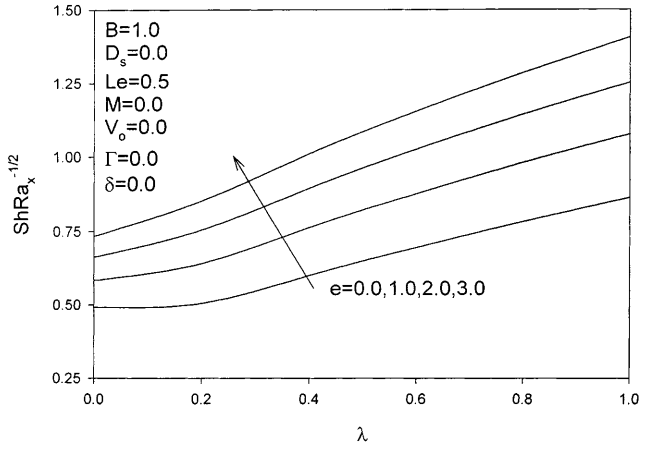

Fig. 11.

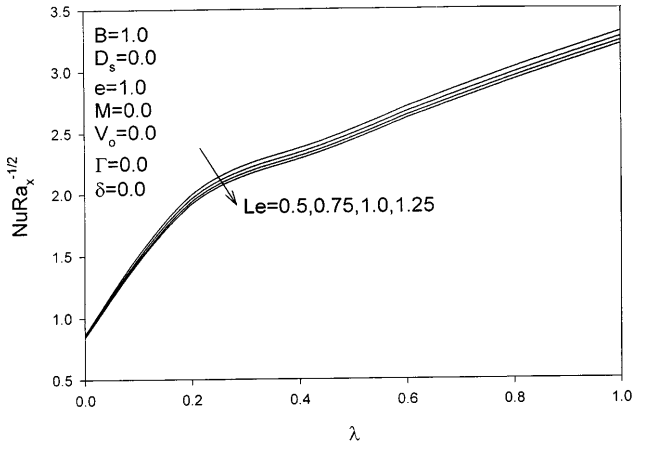

Fig. 12.

wall temperature and concentration as well as free stream temperature were assumed to vary with the vertical distance along plate according to a power-law form. Also, a transverse magnetic field of uniform strength was assumed to exist in the direction normal to that of the flow. The governing equations were developed and transformed using appropriate similarity transformations. The resulting transformed equations were then solved numerically by an implicit, iterative, finite-difference scheme. The obtained results for special cases of the problem were compared with previously published work and found to be in excellent agreement. It was found that while the local Nusselt number decreased as a result of the presence of either the magnetic field, negative free stream temperature stratification or positive wall mass transfer, it increased due to imposition of both negative wall mass transfer and free stream temperature stratification. Also, the Nusselt number was increased due to the presence of heat absorption effects. In addition, the Nusselt number decreased as a result of considering the porous medium inertia effects. Furthermore, increasing the ratio of concentration to thermal buoyancies was found to cause enhancements in the values of the Nusselt number and the Sherwood number. Finally, thermal dispersion was found

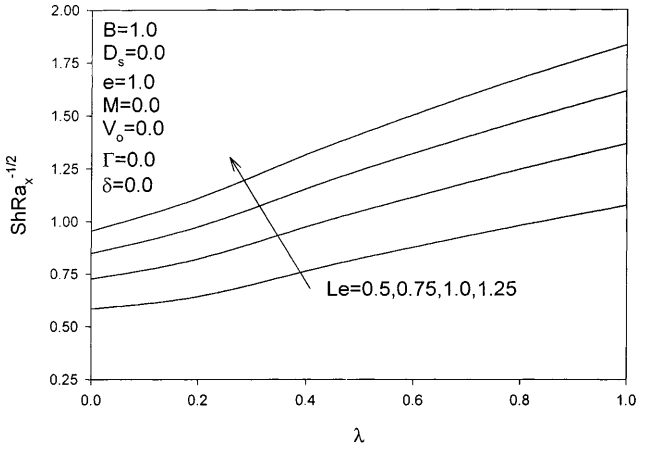

Fig. 13.

to increase the rate of heat transfer from the plate. It is hoped that the present work will serve as a vehicle for understanding more complex problems involving the various physical effects investigated in the present problem.

References

Acharya S; Goldstein RJ (1985) Natural convection in an externally heated vertical or inclined square box containing internal energy sources. ASME J Heat Transfer 107: 855–866

Aldoss TK; Al-Nimr MA; Jarrah MA; Al-Sha'er BJ (1995) Magnetohydrodynamic mixed convection from a vertical plate embedded in a porous medium. Num Heat Transfer 28A: 635–645

Amiri A; Vafai K (1994) Analysis of dispersion effects and non-thermal equilibrium, non-darcian, variable porosity incompressible flow through porous media. Int J Heat Mass Transfer 37: 936–954

Bian W; Vasseur P; Meng F (1996) Effect of electromagnetic field on natural convection in an inclined porous medium. Int J Heat Fluid Flow 17: 36–44

Blottner FG (1970) Finite-difference methods of solution of the boundary-layer equations. AIAA Journal 8: 193–205

Chamkha AJ (1996) Non-Darcy hydromagnetic free convection from a cone and a wedge in porous media. Int Commun Heat Mass Transfer 23: 875–887

Chamkha AJ (1997a) Hydromagnetic natural convection from an isothermal inclined surface adjacent to a thermally stratified porous medium. Int J Eng Sci 35: 975–986

Chamkha AJ (1997b) Non-Darcy fully developed mixed convection in a porous medium channel with heat generation/absorption and hydromagnetic effects. Num Heat Transfer 32: 653–675

Cheng P; Minkowycz WJ (1977) Free convection about a vertical flat plate embedded in a porous medium with application to heat transfer from a dike. J Geophy 82: 2040–2044

Cheng P; Vortmeyer D (1988) Transverse thermal dispersion and wall channeling in a packed bed with forced convective flow. Chemical Eng Sci 43: 2523–2532

Cramer KR; Pai SI (1973) Magnetofluid dynamics for engineers and applied physicists. Scripta Publishing Company, Washington, DC

Garandet JP; Alboussiere T; Moreau R (1992) Driven convection in a rectangular enclosure with a transverse magnetic field. Int J Heat Mass Transfer 34: 741–748

Hunt ML; Tein CL (1988) Non-Darcian convection in cylindrical packed beds. J Heat Transfer 110: 378–384

Gorla RS; Bakir AY; Byrd L (1996) Effects of thermal dispersion and stratification on combined convection on a vertical surface embedded in a porous medium. Transport in Porous Media 25: 275–282

Hsieh JC; Chen TS; Armaly BF (1985) Non-similarity solutions for mixed convection from vertical surfaces in a porous medium. Int J Heat Mass Transfer 36: 1485–1493

Hunt ML; Tein CL (1988) Non-Darcian convection in cylindrical packed beds. J Heat Transfer 110: 378–384

Khanafer K; Chamkha AJ (1998) Hydromagnetic natural convection from an inclined porous square enclosure with heat generation. Num Heat Transfer 33: 891–910

Lai FC; Kulacki FA (1991) Non-Darcy mixed convection along a vertical wall in a saturated porous medium. Int J Heat Mass Transfer 113: 252–255

Minkowycz WJ; Cheng P; Chang CH (1985) Mixed convection about a non-isothermal cylinder and sphere in a porous medium. Num Heat Transfer 8: 349–359

Nakayama A; Koyama H (1987) A general similarity transformation for free, forced and mixed convection in darcy and non-darcy porous media. J Heat Transfer 109: 1041–1045

Plumb OA (1983) Thermal dispersion in porous media heat transfer. ASME/JSME Thermal Conference Proceedings 2: 17–21

Ranganathan P; Viskanta R (1984) Mixed convection boundary layer flow along a vertical surface in a porous medium. Num Heat Transfer 7: 305–317

Rapits A; Massias C; Tzivanidis G (1982a) Hydromagnetic free convection flow through a porous medium between two parallel plates. Phys Lett 90A: 288–289

Rathish KBV; Singh P (1998) Effect of thermal stratification on free convection in a fluid-saturated porous enclosure. Num Heat Transfer 34: 343–356

Vafai K; Tien CL (1981) Boundary and inertia effects on flow and heat transfer in porous media. Int J Heat Mass Transfer 24: 195–203

Vajravelu K; Nayfeh J (1992) Hydromagnetic convection at a cone and a wedge. Int Commun Heat Mass Transfer 19: 701–710

Yagi S; Kunii D; Endo K (1985) Porous medium heat transfer. Int J Heat Mass Transfer 7: 333–339